

Catalytic Activity of Cu/AC Catalyst on Direct Synthesis of 1,1 Dibutoxybutane from 1-Butanol

Yoeswono¹, Mukhamad Faeshol Umam¹, Triyono², Iip Izul Falah²

¹The Education and Training on Oil and Gas, Sorogo Street No. 1, Cepu, Central Java, Indonesia 58315

²Physical Chemistry Laboratory, Chemistry Department, Faculty of Mathematics and Natural Sciences, Universitas Gadjah Mada, Sekip Utara Yogyakarta, Indonesia 55281

INFORMASI NASKAH

Diterima : 24 Juni 2024
Direvisi : 21 Agustus 2024
Disetujui : 26 Agustus 2024
Terbit : 26 Agustus 2024

Email korespondensi:
yoeswono@esdm.go.id

Laman daring:
<https://doi.org/10.37525/mz/2024-1/613>

ABSTRACT

This study was conducted to investigate the catalytic activity of the Cu/AC catalyst in the direct synthesis of 1,1-dibutoxybutane (DBB) from 1-butanol. The Cu/AC catalyst was prepared through dry impregnation and characterized using TG/DTA, XRD, and SEM-EDS. The catalyst was placed in a continuous downflow quartz tube reactor, and 1-butanol was pumped into a preheated reactor under an N₂ atmosphere at a specific temperature, contact time, reaction time, and 1-butanol concentration. The product was condensed and analyzed using FTIR, ¹H, ¹H-¹H COSY, ¹³C NMR, GC-MS, and GC. The results showed that the catalyst preparation procedure successfully impregnated Cu on the AC surface, and the resulting catalyst had catalytic activity in the direct synthesis of DBB from 1-butanol. As the temperature rises, the 1-butanol conversion and DBB selectivity increase. Longer contact and reaction times could lead to higher DBB concentrations. The concentration of 1-butanol in the feed affected the DBB concentration in the finished product. Higher conversion of 1-butanol is possible at a certain concentration. The addition of magnesium to the Cu/AC catalyst improved DBB formation. Although magnesium promoted butanal formation, DBB formation was more favorable on the Cu surface.

Keywords: 1,1-dibutoxybutane, Cu/AC catalyst, dry impregnation, catalytic activity

ABSTRAK

Telah dilakukan serangkaian eksperimen untuk mengkaji aktivitas katalis Cu/AC pada sintesis 1,1-dibutoksibutana (DBB) secara langsung dari 1-butanol. Katalis Cu/AC dibuat dengan teknik pengembunan kering dan dikarakterisasi dengan TG/DTA, XRD, dan SEM-EDS. Sejumlah katalis dimasukkan dalam reaktor kaca tipe aliran ke bawah dan 1-butanol dialirkan ke dalam reaktor yang telah dipanaskan sebelumnya dalam atmosfer N₂ pada temperatur, waktu kontak, waktu reaksi, dan konsentrasi 1-butanol tertentu. Produk yang diperoleh dikondensasikan dan dianalisis dengan FTIR, ¹H, ¹H-¹H COSY & ¹³C NMR, GC-MS, dan GC. Data hasil eksperimen menunjukkan bahwa prosedur preparasi katalis telah berhasil mengembankan Cu pada permukaan karbon aktif dan katalis yang diperoleh memiliki aktivitas katalitik pada sintesis DBB secara langsung dari 1-butanol. Konversi 1-butanol dan selektivitas terhadap DBB meningkat seiring peningkatan temperature. Waktu kontak dan waktu reaksi yang lebih lama dapat meningkatkan perolehan DBB. Konsentrasi 1-butanol dalam umpan mempengaruhi perolehan DBB. Pada konsentrasi 1-butanol tertentu, dapat dihasilkan DBB lebih banyak. Penambahan magnesium pada Cu/AC dapat meningkatkan perolehan DBB. Magnesium meningkatkan pembentukan butanal, namun demikian pembentukan DBB lebih disukai pada permukaan Cu.

Kata kunci: 1,1-dibutoksibutana, katalis Cu/AC, pengembunan kering, aktivitas katalitik.

INTRODUCTION

Feedstocks derived from petroleum are extremely important to the transportation fuel and petrochemical sectors. Petroleum will eventually run out because it is not a renewable resource. It is imperative to increase research into and use of alternative fuels as a supplement to petroleum-derived materials and as a replacement for petrochemical feedstocks. Being a plentiful and renewable source of carbon-containing molecules, biomass offers a possible substitute for traditional liquid fuels and chemicals. Another reason for the development of alternative energies from biomass or oxygenated fuels, which emit less HC and CO than petroleum fuel, is the issue of environmental quality degradation. Two oxygenated fuels that have seen a lot of research and production are biodiesel and bioethanol. The high cetane number (CN) of 1,1-dialkoxyalkane makes it a possible oxygenated fuel additive for diesel engines. The reaction of aldehydes and alcohols on acid catalysts can produce 1,1-dialkoxyalkane. The 1,1-dialkoxyalkane synthesis has made use of strong mineral acids as homogeneous catalysts, including H₂SO₄, HF, HCl, and p-toluenesulphonic acid.

However, these processes have a few drawbacks, including issues with corrosion and product separation. Most of these issues could be solved

by employing a heterogeneous catalyst. Zeolite, zirconium sulfate, montmorillonite, nickel cation, metal halides on solids support, heteropolyacids, oxides/mixed oxides, and ion-exchange resins are some examples of heterogeneous catalysts. The direct synthesis of 1,1-dialkoxyalkane from alcohol decomposition on heterogeneous catalysts has also been documented by Szymanski et al. and Dubois. Because it provides an efficient process, the direct synthesis of 1,1-dialkoxyalkane is an intriguing area to investigate.

1-Butanol is a biofuel that has recently come under scrutiny as a potential substitute for ethanol. One standard method for producing 1-butanol is the chemical Oxo process. This involves reacting propylene with hydrogen and carbon monoxide in a catalyst-supported reaction. The resulting aldehydes are then hydrogenated to produce a mixture of iso- and n-butanols. The ABE fermentation process can also be used to produce 1-butanol from renewable resources, similar to how ethanol is produced. Compared to ethanol, this chemical has a higher energy content, lowers water absorption, and can be used in regular internal combustion engines without any changes as a gasoline blending component. The low CN (17) of this compound makes it unsuitable as a diesel fuel blend component, but 1,1-dibutoxybutane (DBB), its acetal, has a high CN (105) and a boiling point

that falls within the diesel fuel boiling range. Like diesel fuel, DBB has a similar flash point and density. Figure 1 shows the molecular structure of DBB.

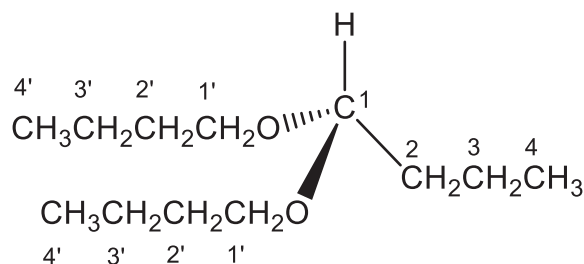


Figure 1. Molecular structure of 1,1-dibutoxybutane (DBB)

While numerous catalysts have been investigated for acetal synthesis, as mentioned earlier, few reports have used a Cu/AC catalyst to synthesize DBB from 1-butanol directly. In order to directly synthesize DBB from 1-butanol, this study employed a Cu/AC catalyst to investigate its catalytic activity concerning temperature, contact time, reaction time, 1-butanol concentration, and the effects of magnesium addition.

METHOD

a. Materials

PT. Bayu Lestari – Indonesia was the supplier of the activated carbon. The following substances were acquired from Merck: copper dichloride dihydrate ($\text{CuCl}_2 \cdot 2\text{H}_2\text{O}$), magnesium dichloride hexahydrate ($\text{MgCl}_2 \cdot 6\text{H}_2\text{O}$), hydrochloric acid (HCl), acetone ($\text{C}_3\text{H}_6\text{O}$), and 1-butanol ($\text{C}_4\text{H}_9\text{OH}$). Both nitrogen (N_2) and hydrogen (H_2) gas were acquired from PT. Samator – Indonesia, where they were purchased.

b. Instrumentations

TG/DTA PerkinElmer Diamond was utilized to determine the adsorption strength of the catalyst as well as other materials that were present on the surface of the activated carbon. In order to determine the crystallinity of the catalyst, an X-ray diffraction (XRD) Shimadzu X-6000 was utilized, with a scan range of $2\theta = 3.02 - 80.00$ and a Cu radiation source. The SEM-EDS JSM-6510 was utilized to carry

out the elemental composition analysis of the catalyst. The GC-MS Shimadzu QP2010S and the GC HP 5890-II were utilized to ascertain the reaction products' composition. A number of different techniques, including FTIR Shimadzu IRPrestige-21, ^1H and $^1\text{H}-^1\text{H}$ COSY NMR JNM-ECZ500R/S1, ^{13}C NMR JNM-ECS400, and GC-MS, were utilized to validate the molecular structure of DBB.

c. Procedure

- Catalysts preparation

After being crushed and sieved, commercial activated carbon (AC-rec) was reduced to a size of 60–80 mesh (0.177–0.250 mm). The AC-rec was subjected to a 12-cycle acetone extraction in a Soxhlet extractor, followed by a 2-hour drying period at 110°C . It was then rinsed with distilled water until an AgNO_3 solution detected no chloride ions, and finally dried for 24 hours at 110°C . (AC-ext.). We reduced the AC-ext. for 3 hours at 300°C using 10% H_2 in N_2 at a total flow rate of 20 mL/min (AC), after which we calcined it for 4 hours at 450°C in a 20 mL/min N_2 atmosphere to get AC-cal. The Cu/AC catalyst was prepared by impregnating AC-ext. with a $\text{CuCl}_2 \cdot 2\text{H}_2\text{O}$ solution using the dry impregnation method, resulting in a 1% (w/w) Cu concentration on activated carbon. Following a 24-hour cooling period at room temperature, the mixture was evaporated at 80°C for 12 hours, dried at 110°C for another 24 hours, and finally subjected to calcination and reduction in the same way as before. The CuMg/AC catalyst was made following the same steps as the Cu/AC preparation, except using a solution of $\text{CuCl}_2 \cdot 2\text{H}_2\text{O}$ and $\text{MgCl}_2 \cdot 6\text{H}_2\text{O}$ in a proportion of 1% (w/w) for Cu and Mg on activated carbon.

- Catalyst activity experiment

A quart tube reactor with an inside diameter of 1 cm and a fixed bed catalyst type that allows for continuous downflow was used to conduct the catalyst activity. The catalyst, weighing 2 g, was fixed in the reactor's center using rock wool at both ends for every experiment. The reactor was placed

in a programmed temperature furnace with its inlet portion approximately 20 cm inside the heating area to avoid a temperature gradient when the reactant came into contact with the catalyst. The catalyst had to be heated in a furnace under a N₂ atmosphere at a rate of 5 °C/min for at least 30 minutes to get it to the right temperature. After pumping the reactant into the reactor, a 1.5 mL eppendorf tube was placed inside a 50 mL impinger tube to collect the condensed product. For subsequent testing, the gathered material was consistently frozen. Applying GC-MS and GC, we could ascertain the product's conversion and distribution.

We varied the temperature from 250 to 450 °C while keeping the 1-butanol to N₂ flow rate ratio constant at 1:1 and the total flow rate at 20 mL/min to determine the effect of temperature on the catalytic activity. By changing the contact time to 0.06, 0.09, and 0.18 minutes while maintaining a constant flow rate ratio of 1-butanol to N₂ at 1:1, we were able to assess the impact of contact time on catalytic activity. The impact of reaction time on catalytic activity was assessed by sampling at 30-minute intervals from 25 to 145 minutes apart, maintaining a 1:1 ratio of 1-butanol to N₂, and a total flow rate of 20 mL/min. By changing the 1-butanol flow rate ratio to the total flow rate from 0.25 to 0.37 while keeping the total flow rate constant at 40 mL/min, we were able to assess the impact of different 1-butanol concentrations on the catalytic activity experiment. By maintaining a constant ratio of 1-butanol to N₂ at 1:1 and a total flow rate of 20 mL/min, the CuMg/AC catalyst was heated to 450 °C in order to assess the impact of Mg addition on the catalytic activity.

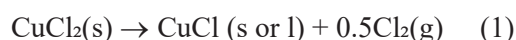
RESULTS AND DISCUSSION

A. Catalyst characterization

- TG/DTA analysis

The sample was heated in a nitrogen atmosphere at a rate of 5 °C/min from 30 to 1000 °C for TG/DTA analysis of pure CuCl₂·2H₂O, AC-ext, and CuCl₂·2H₂O/AC-ext. The results are displayed in Figure 2.

The dehydration process caused a mass loss of 21.03% (4.080 mg) as shown in the TG/DTA curve of CuCl₂·2H₂O (Figure 2(a)), which peaked at 105 °C. Like what Galwey and Brown had previously reported, the dehydration of CuCl₂·2H₂O (Figure 2(a)) happened in a single step. Two endothermic peaks, corresponding to mass losses of 15.11% (2.932 mg) and 4.48% (0.869 mg), are visible on the TGA curve at 441 °C and 468 °C, respectively. These peaks were observed due to the phase transition from solid to liquid CuCl that occurred during the decomposition of CuCl₂ as demonstrated in the reaction (1). The melting point of the CuCl is 430 °C. A small amount of liquid CuCl may have volatilized during the phase change at 468 °C, which would explain the small mass loss.



The subsequent 34.32% mass loss, or 6.658 mg, over the temperature range of 481-639 °C may have been caused by the breakdown of CuCl to produce Cu metallic. At this point, it's possible that CuCl vaporization is to blame for the discrepancy between the calculated and observed masses remaining (Table 1). In this case, XRD analysis would prove that Cu metallic phases had formed.

Table 1. Thermal decomposition of CuCl₂·2H₂O

Species	Mass remaining/%	
	Calculated	Observed
CuCl ₂ ·2H ₂ O	100.00	100.00
CuCl ₂	78.86	78.97
CuCl	58.07	59.37
Cu	37.27	25.05

Figure 2(b) displays the outcome of the TG/DTA analysis of CuCl₂·2H₂O/AC-ext. The dehydration process results in a peak at 68 °C with an endothermic temperature and a 6.86% mass loss, or 1.609 mg. Across the temperature range of 276-915 °C (20.814 mg), a significant mass loss of 88.77% is noted. The decomposition of CuCl₂ and lignin by the activated carbon, which occurred at

lower temperatures than in Figure 2 (a) and (c), may have contributed to this mass loss. The temperature at which lignin decomposes was reduced by adding $\text{CuCl}_2 \cdot 2\text{H}_2\text{O}$ to the surface of the activated carbon. Both the melting and decomposition temperatures of CuCl_2 were reduced as a result. Atoms close to the surface need less energy to escape the solid phase because there are fewer bonds and cohesive energy.

According to Figure 2 (c), the degradation of the activated carbon's lignin began at temperatures around $300\text{ }^\circ\text{C}$ and persisted for the duration of the subsequent temperature observations. According to Viswanathan et al., lignin decomposition occurred between 280 and $550\text{ }^\circ\text{C}$.

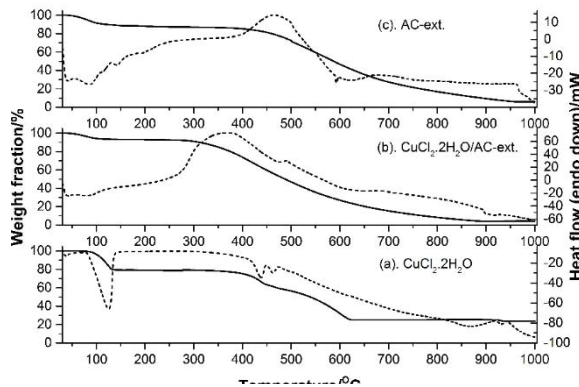


Figure 2. TG/DTA analysis result of catalyst studied

- **X-ray diffraction analysis**

In Figure 3, we can see the catalyst's XRD spectra. At $2\theta = 9.0$ and 23.5° , two wide diffraction peaks exist in the XRD spectra. These wide peaks indicate that the lignin in question has an amorphous structure and was partially decomposed between 280 and $550\text{ }^\circ\text{C}$. A turbostratic carbon structure was formed during the carbonization step of activated carbon synthesis, as indicated by the diffraction peak at $2\theta = 43.8^\circ$. Figure 3 (b) displays the Cu/AC catalyst's diffraction peaks. Two Cu diffraction peaks are observed at $2\theta = 43.2^\circ$ and 50.3° . Crystallography Open Database (COD) confirmed these diffraction peaks with the Match! Version 2.3.3 program.

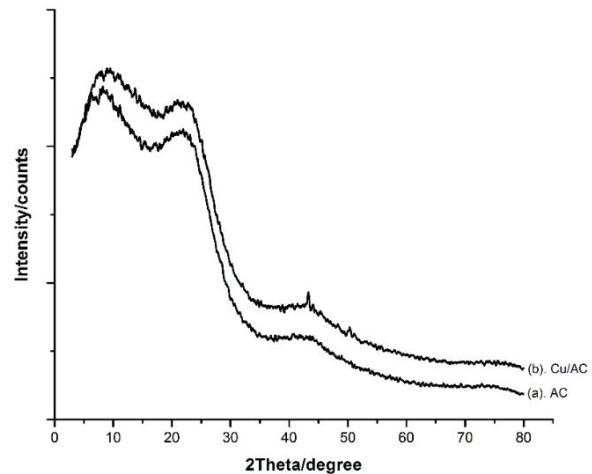
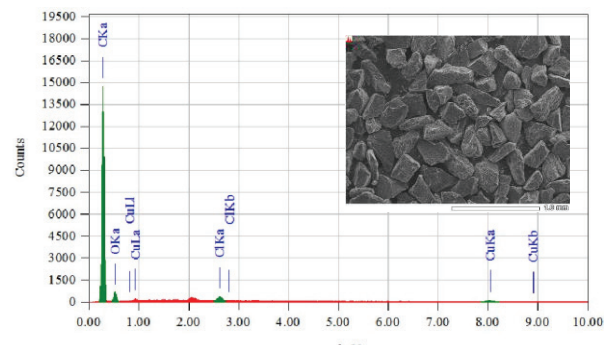


Figure 3. X-ray diffraction spectra of the Cu/AC catalyst

The results of the TG/DTA and XRD analyses suggest that the catalyst preparation process successfully impregnated the activated carbon with Cu metal.

- **SEM-EDS analysis**

Figure 4 shows the outcome of the SEM-EDS JSM-6510 analysis of the catalyst's elemental composition. The activated carbon had copper impregnated onto it according to the catalyst preparation process, but chloride-containing species were still adsorbed onto the surface, according to the SEM-EDS results. The observed Cu to Cl ratio of 1.4167 in fresh catalyst, which is greater than the calculated Cu to Cl ratio of 0.8962 in CuCl_2 , indicates the presence of Cu. These EDS results corroborated the XRD data.



Element	Mass/%
C	82.54
O	15.38
Cl	0.54
Cu	1.53
Total	100.00

Figure 4. Elemental composition analysis of Cu/AC catalyst by SEM-EDS

B. Catalytic Activity

An experiment was carried out without the catalyst (in an empty reactor). The product was analyzed using GC-MS to guarantee that the catalytic activity was solely due to the catalyst. 1.20% of the original 1-butanol was converted into 1-butene, 0.09% into butanal, 0.25% into 1-butylbutanoate, 0.70% into DBB, and 0.05% into other small products. The results suggest that the reactor did not play a major role in the experiment's catalytic activity.

- Molecular structure confirmation of DBB

The presence of the DBB compound in the product was confirmed using FTIR, ¹H-NMR, ¹³C-NMR, and GC-MS techniques. To prepare the sample, the product was distilled just below the boiling point temperature of DBB (215.8 °C), and the remaining residue in the distilling flask was collected for further analysis. Figure 5 displays the FTIR spectra of the compound in the residue sample. The peaks observed at approximately 2932 and 2870 cm⁻¹ correspond to the stretching of C-H bonds in methyl and methylene groups. The peaks at around 1458 cm⁻¹ (C-H bends of methylene groups) and 1381 cm⁻¹ (C-H bends of methyl groups) provide further evidence for these functional groups. Furthermore, the presence of peaks at approximately 1126 and 1072 cm⁻¹ indicates the presence of asymmetrical and symmetrical C-O-C stretches in the compound's molecular structure.

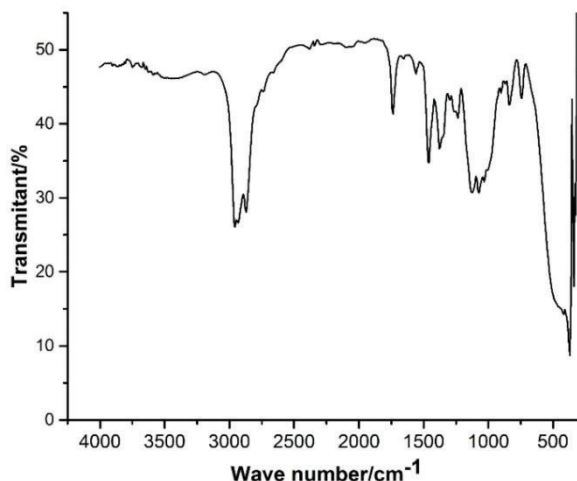


Figure 5. FTIR spectra of the residue sample from distillation of the decomposition product of 1-butanol on Cu/AC catalyst

The residue sample's ¹H NMR spectra are displayed in Figure 6, and the sequence of the unshielded proton chemical shift is described below. ¹H NMR (400 MHz, Chloroform-d) (/ppm: 0.88 (t, J=7.33 Hz, 9 H, 4-CH₃ and 4'-CH₃×2), 1.27 - 1.39 (m, 6 H, 3-CH₂ and 3'-CH₂×2), 1.46 - 1.58 (m, 6 H, 2-CH₂ and 2'-CH₂×2), 3.36 (dt, J=9.39, 6.75 Hz, 2 H, 1'-CHa), 3.53 (dt, J=9.39, 6.75 Hz, 2 H, 1'-CHb), 4.43 (t, J=5.72 Hz, 1 H, 1-CH). Since the protons at 1'-C (Ha and Hb) are diastereotopic, they couple with each other (through two bonds) and appear at different chemical shifts.

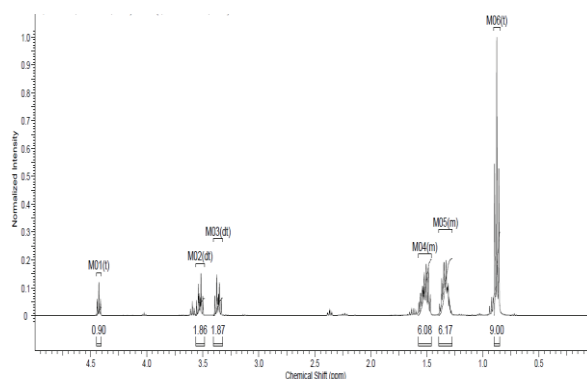


Figure 6. ¹H-NMR spectra of the residue sample from the distillation of the decomposition product of 1-butanol on Cu/AC catalyst

Figure 7 shows the result of the investigation into proton-proton correlations using Proton-Proton Correlation Spectroscopy (^1H - ^1H COSY) NMR. Two sets of proton concentrations, 0.88 ppm for methyl and 1.27-1.39 ppm for methylene, were found to be correlated. At 1.46-1.58 ppm, there was a correlation between these three groups of methylene protons. The 336 and 3.53 ppm diastereotopic proton sets correlated with the 1.46-1.58 ppm methylene proton sets, and the 4.43 ppm methine proton set correlated with the remaining 1.46-1.58 ppm methylene proton sets.

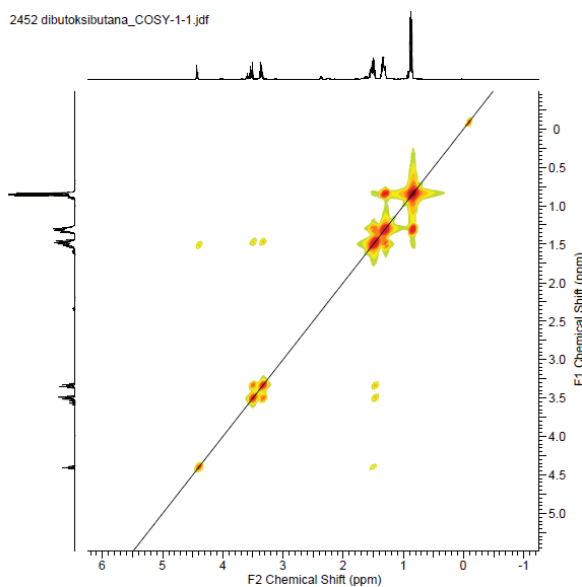


Figure 7. ^1H - ^1H COSY NMR spectra of the residue sample from the distillation of the decomposition product of 1-butanol on Cu/AC catalyst

Compound ^{13}C -NMR spectra from the residue sample and the corresponding data are displayed in Figure 8. 13.97 (s, 2 C, 4 $^\circ$ -CH $_3$ Ö2), 14.03 (s, 1 C, 4-CH $_3$), 18.19 (s, 1 C, 3-CH $_2$), 19.51 (s, 2 C, 3 $^\circ$ -CH $_2$ ×2), 32.06 (s, 2 C, 2 $^\circ$ -CH $_2$ ×2), 35.62 (s, 1 C, 2-CH $_2$), 65.14 (s, 2C, 1 $^\circ$ -CH $_2$ O×2), and 102.95 (s, 1 C, 1-acetal-C) were detected by ^{13}C -NMR (101 MHz, Chloroform-d). It was also reported by Kamizono et al. that a similar outcome had occurred. In agreement with Silverstein et al., there was acetal carbon at a chemical shift of 102.95 ppm.

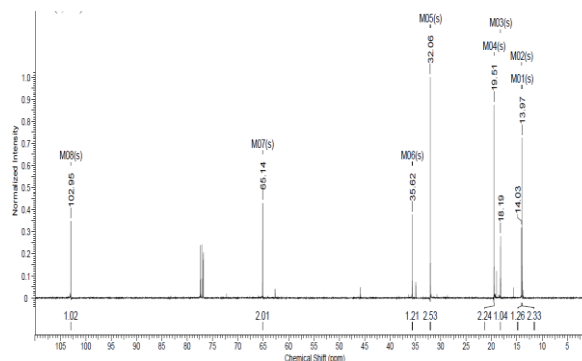
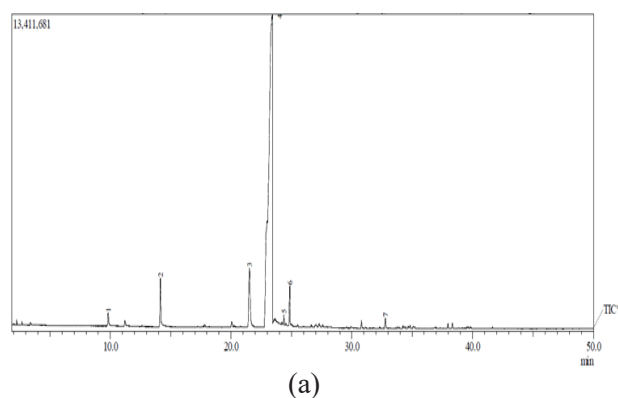


Figure 8. ^{13}C -NMR spectra of the residue sample from the distillation of the decomposition product of 1-butanol on Cu/AC catalyst

The GC-MS analysis result of the residue sample is depicted in Figure 9. The compound identified as DBB exhibits the highest peak in Figure 9(a) with a retention time of 23.400 minutes. The presence of minor peaks in the chromatogram suggests the presence of impurities in the sample, with a combined concentration of 12.25%. The compound observed at a retention time of 23.400 minutes exhibits fragmentations with the following mass-to-charge ratios (m/z): 202 [M] $^+$ (calculated for C $_{12}$ H $_{16}$ O $_2$, 202.33), 159 [M - C $_3$ H $_7$] $^+$, 129 [M - C $_4$ H $_9$ O] $^+$, 73 [M - C $_4$ H $_9$ OCH(C $_3$ H $_7$)] $^+$, and 57 (base peak) [M - C $_4$ H $_9$ OCH(C $_3$ H $_7$)O] $^+$ (Figure 9 (b)). These fragments exhibited typical features of the acetal structure. Based on FTIR, ^1H -NMR, ^1H - ^1H COSY NMR, ^{13}C -NMR, and GC-MS data, the structure of the compound in the residue sample is concluded to be DBB.



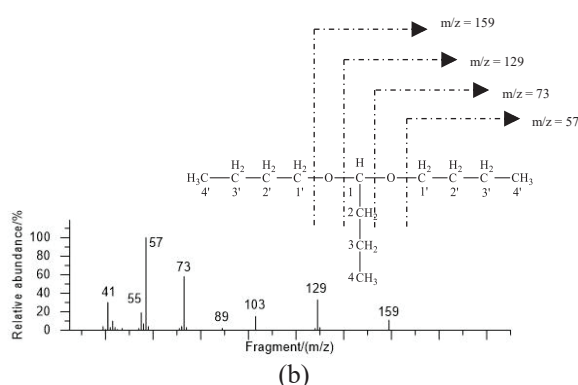
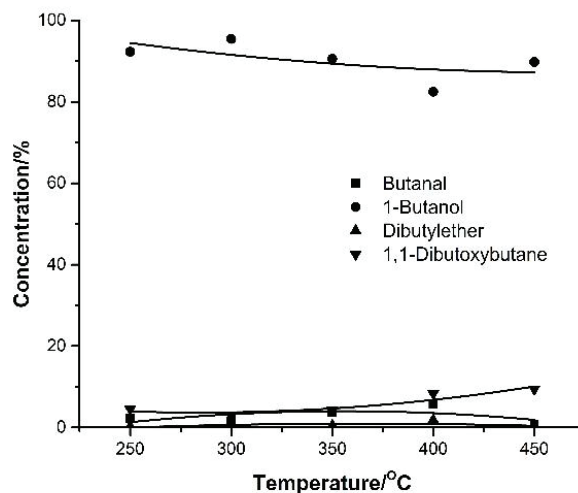


Figure 9. GC-MS analysis result of the residue sample from distillation of the decomposition product of 1-butanol on Cu/AC catalyst

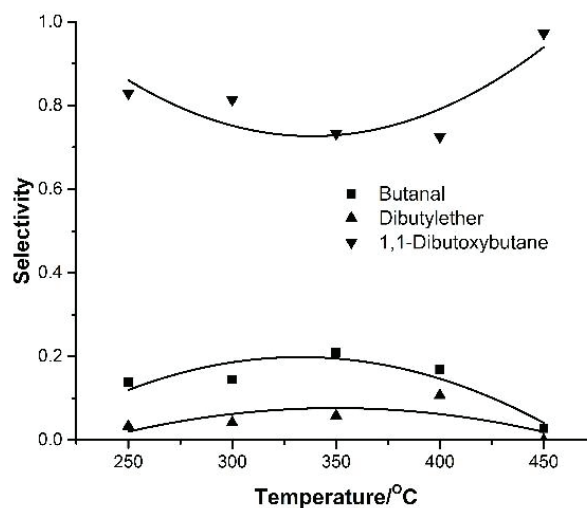
Temperature Effect

The dependence of 1-butanol conversion and DBB selectivity on temperature in the presence of Cu/AC catalyst are presented in Figure 10. The conversion of 1-butanol on Cu/AC catalyst increases as temperature increases in Figure 10(a). The Cu/AC catalyst could give high selectivity toward DBB formation (Figure 10(b)) up to 0.97 (450 °C), and the selectivity increases as temperature increases.

Butanal selectivity decreased after DBB selectivity increased. In a typical acid-catalyzed reaction, two moles of monohydric alcohol and one mole of aldehyde can be converted into acetal. After a dehydrogenation reaction, the corresponding alcohols can be converted into aldehydes. Achieving the high DBB selectivity would depend on the effectiveness of the reaction between the formed butanal and 1-butanol. In simpler terms, the DBB is the outcome of a secondary reaction between the n-butanol and the butanal that have been formed at the active sites. While studying the breakdown of ethanol on activated carbon, Szymanski et al. also noted this phenomenon.



(a)



(b)

Figure 10. Dependence of conversion (a) and selectivity (b) on the temperature in the decomposition of 1-butanol on Cu/AC

Contact time effect

In Figure 11, we can see how the contact time affects the 1-butanol decomposition on Cu/AC. Increasing the duration of contact resulted in a higher concentration of DBB. A DBB concentration of 9.40% at 450 °C was achieved with an extended contact time of 0.18 minutes. Since copper's antibonding state is filled and lies below Fermi energy,

the adsorbate-Cu interaction is weak but still slightly attractive. Increasing the temperature initiates molecular rearrangement or bond breaking on the surface while increasing the contact time increases the likelihood of Cu and adsorbate interaction for subsequent reactions. The assertions were backed by the fact that the concentration of DBB increased with increasing contact time and temperature.

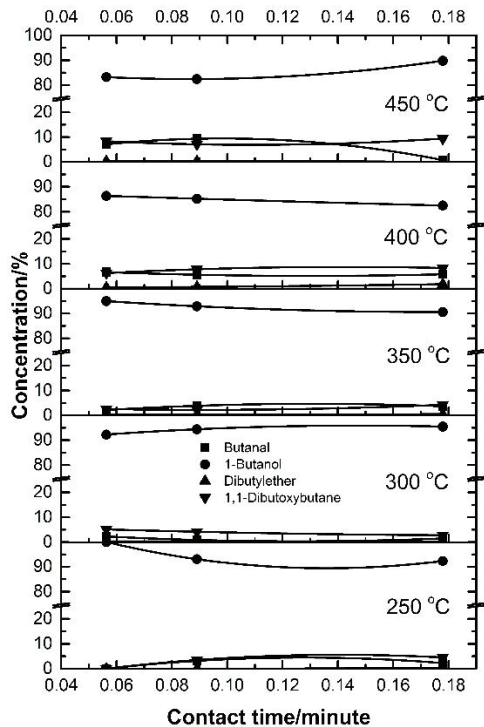


Figure 11. Dependence of conversion on contact time in the decomposition of 1-butanol on Cu/AC catalyst

- **Reaction time effect**

Figure 12 shows the conversion-reaction time dependence of 1-butanol decomposition on the Cu/AC. While the conversion of 1-butanol on Cu/AC catalyst increases at higher temperatures, it decreases at lower ones as reaction time increases. The DBB concentration was 25.53% at 450 °C, with the maximum reaction time being 145 minutes. Longer reaction times and higher temperatures were favorable for 1-butanol decomposition on Cu/AC catalyst. An increase in temperature triggers molecular rearrangement or bond breaking on the surface, while a longer reaction time allows for more reactants to be adsorbed on the Cu

surface, increasing the interaction probability between the butanal and 1-butanol that are formed to form DBB.

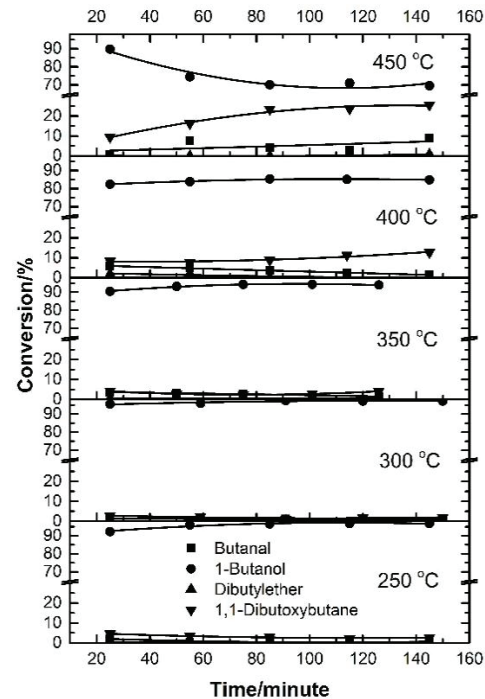


Figure 12. Dependence of conversion on reaction time in decomposition of 1-butanol on Cu/AC catalyst

- **1-Butanol concentration effect**

Figure 13 shows that the 1-butanol conversion is most favorable at low concentrations in the feed and decreases at high concentrations. At 450 °C, a 1-butanol conversion of 22.94% and a DBB concentration of 13.14% were achieved with a 1-butanol concentration of 0.36 (measured as the ratio of 1-butanol to total flow rate). It suggests that if there were enough reactants adsorbed on the active sites, the butanal would be able to desorb from the pores and re-adsorb on the outer surface of the active sites more easily, increasing the likelihood that it would interact with 1-butanol, leading to a higher conversion of 1-butanol. According to Szymanski et al., acetal's favorable surface formation was facilitated by its relatively small molecular size. Desorption of formed butanal from pores thus limited the rate of DBB formation. Butanal will take longer to desorb from pores when the concentration of 1-butanol is higher

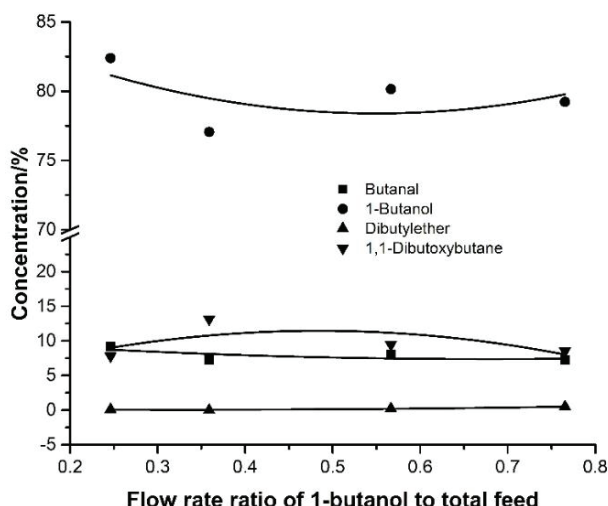


Figure 13. Dependence of conversion on 1-butanol concentration in decomposition of 1-butanol on Cu/AC catalyst at 450 °C

Mg addition effect

Figure 10 shows that the addition of magnesium significantly affects the distribution of products from the decomposition of 1-butanol.

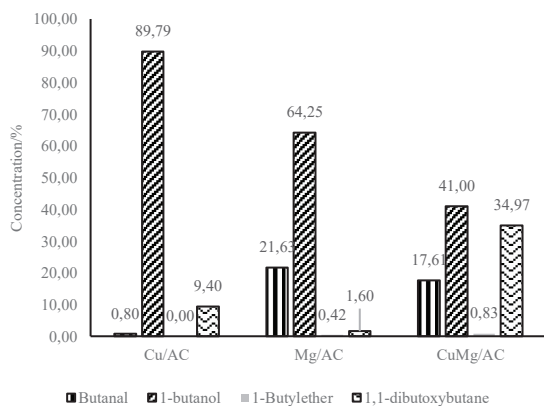


Figure 14. Effect of Mg addition on product distribution at 450°C

With the Mg/AC catalyst, achieving a higher butanal concentration was possible. The results show magnesium is more active than Cu/AC catalyst in 1-butanol dehydrogenation. The dehydrogenation process and the formation of acetals can be accelerated by adding magnesium to the Cu/AC catalyst. Coadsorbed alkali atoms significantly lower the dissociation activation barrier. However, low DBB formation on Mg/

AC demonstrated that magnesium alone does not efficiently facilitate acetal formation. We can infer that Mg promotes butanal and DBB formation on the Cu catalyst's surface, which is advantageous. When using a CuMg/AC catalyst at 450 °C, the highest possible concentration of DBB that could be achieved is 34.97%.

CONCLUSION

The Cu/AC catalyst can be used to directly synthesize DBB from 1-butanol, with butanal and dibutyl ether as minor side products. The 1-butanol conversion and DBB selectivity are affected by temperature, contact time, reaction time, and 1-butanol concentration. Magnesium promotes butanal formation. However, DBB formation was favorable on Cu surface. In this study, the maximum concentration of DBB that could be obtained is 34.97% on CuMg/AC catalyst at 450 °C

REFERENCES

Agirre, I., Barrio, V. L., Güemez, B., Cambra, J. F., & Arias, P. L. (2011). Catalytic reactive distillation process development for 1,1 diethoxy butane production from renewable sources. *Bioresource Technology*, 102(2), 1289–1297. doi:10.1016/j.biortech.2010.08.064

Agirre, I., Güemez, M. B., Ugarte, A., Reques, J., Barrio, V. L., Cambra, J. F., & Arias, P. L. (2013). Glycerol acetals as diesel additives: Kinetic study of the reaction between glycerol and acetaldehyde. *Fuel Processing Technology*, 116, 182–188. doi:10.1016/j.fuproc.2013.05.014

Antoniammal, P., & Arivuoli, D. (2012). Size and Shape Dependence on Melting Temperature of Gallium Nitride Nanoparticles. *Journal of Nanomaterials*, 2012, 1–11. doi:10.1155/2012/415797

Catalyst for the selective terminal oxidation of alkanes. (2011). *Focus on Catalysts*, 2011(2), 7–8. doi:10.1016/s1351-4180(11)70050-2

De Micco, G., Bohé, A. E., & Pasquevich, D. M. (2007). A thermogravimetric study of copper chlorination. *Journal of Alloys and Compounds*, 437(1–2), 351–359. doi:10.1016/j.jallcom.2006.08.003

Dunn, A. S. (1994). *Introduction to physical polymer science* (2nd edition). By L. H. Sperling, New York, 1992 John Wiley & Sons Inc. John Wiley & Sons Inc., New York, 1992. pp. xxvii + 594, price £55.00. ISBN 0-471-53035-2. *Polymer International*, 33(2), 233–233. doi:10.1002/pi.1994.210330214

- Frusteri, F., Spadaro, L., Beatrice, C., & Guido, C. (2007). Oxygenated additives production for diesel engine emission improvement. *Chemical Engineering Journal*, 134(1–3), 239–245. doi:10.1016/j.cej.2007.03.042
- Graça, N. S., Pais, L. S., Silva, V. M. T. M., & Rodrigues, A. E. (2010). Oxygenated Biofuels from Butanol for Diesel Blends: Synthesis of the Acetal 1,1-Dibutoxyethane Catalyzed by Amberlyst-15 Ion-Exchange Resin. *Industrial & Engineering Chemistry Research*, 49(15), 6763–6771. doi:10.1021/ie901635j
- Green, S. K. (2004). ELSI and bioterrorism countermeasures? *Nature Biotechnology*, 22(6), 656–656. doi:10.1038/nbt0604-656a
- Güemez, M. B., Requies, J., Agirre, I., Arias, P. L., Barrio, V. L., & Cambra, J. F. (2013). Acetalization reaction between glycerol and n-butyraldehyde using an acidic ion exchange resin. Kinetic modelling. *Chemical Engineering Journal*, 228, 300–307. doi:10.1016/j.cej.2013.04.107
- Hartati, H., Santoso, M., Triwahyono, S., & Prasetyoko, D. (2013). Activities of Heterogeneous Acid-Base Catalysts for Fragrances Synthesis: A Review. *Bulletin of Chemical Reaction Engineering & Catalysis*, 8(1), 14–33. doi:10.9767/brec.8.1.4394.14-33
- Hong, X., McGiveron, O., Kolah, A. K., Orjuela, A., Peereboom, L., Lira, C. T., & Miller, D. J. (2013). Reaction kinetics of glycerol acetal formation via transacetalization with 1,1-diethoxyethane. *Chemical Engineering Journal*, 222, 374–381. doi:10.1016/j.cej.2013.02.023
- Icha, A. (2011). Book Review. *Pure and Applied Geophysics*, 169(7), 1325–1327. doi:10.1007/s00024-011-0442-8
- Kamizono, T., Ohtsuka, A., Hashimoto, F., & Hayashi, K. (2013). Dibutoxybutane Suppresses Protein Degradation and Promotes Growth in Cultured Chicken Muscle Cells. *The Journal of Poultry Science*, 50(1), 37–43. doi:10.2141/jpsa.0120063
- Kinnel, R. B. (2005). *The Systematic Identification of Organic Compounds*, 8th Edition By R. Shriner, C. Hermann, T. Morrill, D. Curtin, and R. Fuson. John Wiley & Sons, Inc., Hoboken, NJ. 2004. ix + 723 pp. 21 × 32 cm. \$102.95. ISBN 0-471-21503-1. *Journal of Natural Products*, 68(2), 309–310. doi:10.1021/np058223w
- Kolasinski, K. W. (2012). *Surface Science*. doi:10.1002/9781119941798
- Kotai, L., Szeplvolgyi, J., Szilagyi, M., Zhibin, L., Baiquan, C., Sharma, V., & K., P. (2013, March 20). Biobutanol from Renewable Agricultural and Lignocellulose Resources and Its Perspectives as Alternative of Liquid Fuels. *Liquid, Gaseous and Solid Biofuels - Conversion Techniques*. doi:10.5772/52379
- Nanda, M. R., Yuan, Z., Qin, W., Ghaziaskar, H. S., Poirier, M.-A., & Xu, C. (charles). (2014). A new continuous-flow process for catalytic conversion of glycerol to oxygenated fuel additive: Catalyst screening. *Applied Energy*, 123, 75–81. doi:10.1016/j.apenergy.2014.02.055
- Niemisto, J., Saavalainen, P., Pongracz, E., & Keiski, R. L. (2013). Biobutanol as a Potential Sustainable Biofuel - Assessment of Lignocellulosic and Waste-based Feedstocks. *Journal of Sustainable Development of Energy, Water and Environment Systems*, 1(2), 58–77. doi:10.13044/j.sdwes.2013.01.0005
- Nørskov, J. K., Studt, F., Abild-Pedersen, F., & Bligaard, T. (2014). *Fundamental Concepts in Heterogeneous Catalysis*. doi:10.1002/9781118892114
- Othman, M. F., Abdullah, H., Sulaiman, N. A., & Hassan, M. Y. (2013). Performance evaluation of an actual building air-conditioning system. *IOP Conference Series: Materials Science and Engineering*, 50, 012051. doi:10.1088/1757-899x/50/1/012051
- Part B Thermal decompositions of selected ionic solids. (1999). *Thermal Decomposition of Ionic Solids*, p. 215. doi:10.1016/s0167-6881(99)80008-1
- Rahaman, M., Graça, N. S., Pereira, C. S. M., & Rodrigues, A. E. (2015). Thermodynamic and kinetic studies for synthesis of the acetal (1,1-diethoxybutane) catalyzed by Amberlyst 47 ion-exchange resin. *Chemical Engineering Journal*, 264, 258–267. doi:10.1016/j.cej.2014.11.077
- Silva, V. M. T. M., & Rodrigues, A. E. (2006). Kinetic studies in a batch reactor using ion exchange resin catalysts for oxygenates production: Role of mass transfer mechanisms. *Chemical Engineering Science*, 61(2), 316–331. doi:10.1016/j.ces.2005.07.017
- Silva, V. M. T. M., Pereira, C. S. M., Rodrigues, A. E., Verevkin, S. P., Emel'yanenko, V. N., Garist, I. V., & Gmehling, J. (2012). Experimental and Theoretical Study of Chemical Equilibria in the Reactive Systems of Acetals Synthesis. *Industrial & Engineering Chemistry Research*, 51(39), 12723–12729. doi:10.1021/ie301484y
- Szymański, G. S., Rychlicki, G., & Terzyk, A. P. (1994). Catalytic conversion of ethanol on carbon catalysts. *Carbon*, 32(2), 265–271. doi:10.1016/0008-6223(94)90189-9
- Viswanathan, B., Neel, P. I., & Varadarajan, T. K. (2009). Development of Carbon Materials for Energy and Environmental Applications. *Catalysis Surveys from Asia*, 13(3), 164–183. doi:10.1007/

s10563-009-9074-8

- Wang, Z., Marin, G., Naterer, G. F., & Gabriel, K. S. (2014). Thermodynamics and kinetics of the thermal decomposition of cupric chloride in its hydrolysis reaction. *Journal of Thermal Analysis and Calorimetry*, 119(2), 815–823. doi:10.1007/s10973-014-3929-6
- Yanowitz, J., Ratcliff, M., McCormick, R., Taylor, J., & Murphy, M. (2014). *Compendium of Experimental Cetane Numbers*. doi:10.2172/1150177